Original Article

Diagnostic performance of computational fluid dynamics (CFD)-based fractional flow reserve (FFR) derived from coronary computed tomographic angiography (CCTA) for assessing functional severity of coronary lesions

Jun Jiang[1#], Changqing Du[2#], Yumeng Hu[3#^], Hong Yuan[4], Jianhua Wang[5], Yibin Pan[6], Lifang Bao[7], Liang Dong[1], Changling Li[1], Yong Sun[1], Xiaochang Leng[3], Jianping Xiang[3], Lijiang Tang[2], Jian'an Wang[1]

[1]Department of Cardiology, The Second Affiliated Hospital, Zhejiang University School of Medicine, Hangzhou, China; [2]Department of Cardiology, Zhejiang Hospital, Hangzhou, China; [3]ArteryFlow Technology Co., Ltd., Hangzhou, China; [4]Department of Cardiology, The First People's Hospital of Linping District, Hangzhou, China; [5]Department of Radiology, The Affiliated Hospital of Medical School, Ningbo University, Ningbo, China; [6]Department of Cardiovascular Medicine, Jinhua Municipal Central Hospital, Jinhua, China; [7]Department of Electrophysiology, Jinhua Municipal Central Hospital, Jinhua, China

Contributions: (I) Conception and design: All authors; (II) Administrative support: JA Wang, L Tang, J Xiang; (III) Provision of study materials or patients: J Jiang, C Du; (IV) Collection and assembly of data: All authors; (V) Data analysis and interpretation: Y Hu, H Yuan; (VI) Manuscript writing: All authors; (VII) Final approval of manuscript: All authors.

[#]These authors contributed equally to this work.

Correspondence to: Jianping Xiang, PhD. ArteryFlow Technology Co., Ltd., 459 Qianmo Road, Hangzhou 310051, China. Email: jianping.xiang@arteryflow.com; Lijiang Tang, MD. Department of Cardiology, Zhejiang Hospital, 12 Lingyin Road, Hangzhou 310013, China. Email: zjyytang@163.com; Jian'an Wang, MD. Department of Cardiology, The Second Affiliated Hospital of Zhejiang University School of Medicine, 88 Jiefang Road, Hangzhou 310009, China. Email: wangjianan111@zju.edu.cn.

Background: Fractional flow reserve (FFR) is the gatekeeper for lesion-specific revascularization decision-making in patients with stable coronary artery disease (CAD). The potential of noninvasive calculation of FFR from coronary computed tomographic angiography (CCTA) to identify ischemia-causing lesions has not been sufficiently assessed. The objective of this study was to evaluate the feasibility and diagnostic accuracy of a novel computational fluid dynamics (CFD)-based technology, termed as AccuFFRct, for the diagnosis of functionally significant lesions from CCTA, using wire-based FFR as a reference standard.

Methods: A total of 191 consecutive patients who underwent CCTA and FFR measurement for suspected or known CAD were retrospectively enrolled at 2 medical centers. Three-dimensional anatomic model of coronary tree was extracted from CCTA data, CFD was applied subsequently with a novel strategy for the computation of FFR in a blinded fashion by professionals. Results were compared to invasive FFR, a threshold of ≤0.80 was used to indicate the hemodynamically relevant stenosis.

Results: On a per-patient basis, the overall accuracy, sensitivity, specificity of AccuFFRct for detecting ischemia were 91.78% (95% CI: 86.08% to 95.68%), 92.31% (95% CI: 81.46% to 97.86%) and 91.49% (95% CI: 83.92% to 96.25%), respectively; those for per-vessel basis were 91.05% (95% CI: 86.06% to 94.70%), 92.73% (95% CI: 82.41% to 97.98%) and 90.37% (95% CI: 84.10% to 94.77%), respectively. The AccuFFRct and FFR was well correlated on per-patient (r=0.709, P<0.001) and per-vessel basis (r=0.655, P<0.001). The AUC of AccuFFRct determination was 0.935 (95% CI: 0.881 to 0.969) and 0.927 (95% CI: 0.880 to 0.960) on per-patient and per-vessel basis.

^ ORCID: 0000-0002-0779-9172.

Conclusions: This novel CFD-based CCTA-derived FFR shows good diagnostic performance for detecting hemodynamic significance of coronary stenoses and may potentially become a new gatekeeper for invasive coronary angiography (ICA).

Keywords: Coronary computed tomographic angiography (CCTA); fractional flow reserve (FFR); computational fluid dynamics (CFD); computed tomographic FFR

Submitted May 24, 2022. Accepted for publication Jan 04 2023. Published online Feb 06, 2023.
doi: 10.21037/qims-22-521
View this article at: https://dx.doi.org/10.21037/qims-22-521

Introduction

Coronary artery disease (CAD) is the most prominent cause of death globally, leading to nearly 9 million deaths annually worldwide (1). Visual inspection of the anatomical stenoses through the coronary angiography and measurement of fractional flow reserve (FFR) are two primary approaches used for evaluating the hemodynamic significance of coronary stenoses (2,3). Although coronary computed tomographic angiography (CCTA) shows good diagnostic performance for detecting and excluding CAD, the correlation between CCTA detected stenosis and myocardial ischemia is unreliable (4). FFR, on the other hand, enables functional assessment of coronary lesions, has emerged as the gold standard for identifying ischemia-causing stenoses (5). Numerous randomized studies have documented superior clinical outcomes for FFR-guided percutaneous coronary intervention (PCI) in patients with stable CAD (6-9). However, the clinical adoption of FFR has been slow all around the world (10). A technique that could fast compute FFR without the need for an expensive pressure wire or hyperemic agent would be beneficial to a wider population.

In recent years, development within the domain of modeling and computational fluid dynamics (CFD) enables simulation of blood flow in coronary arteries and calculation of FFR (11). This FFR value can be obtained from standard acquired CCTA images alone without the need for special imaging protocols or medication administration. The most famous CT-FFR approach (FFR_{CT}, HeartFlow, Redwood City, California, USA) has shown good diagnostic accuracy for detecting significant functional CAD and prognostic value for guiding clinical strategies (12-16). However, FFRCT has very high computational demands, off-site parallel supercomputers are required in the calculation procedure, which limited its widespread clinical application (17).

A novel CFD-based approach (AccuFFRct, ArteryFlow, Hangzhou, China) that allows rapid determination of FFR from CCTA was recently developed. With the AI-assisted three-dimensional (3D) reconstruction technique and a self-developed specific CFD solver for coronary tree, AccuFFRct showed promising diagnostic accuracy for evaluating coronary stenoses in a time-efficient way. However, it has not been adequately examined. Thus, the purpose of this study was to investigate both the feasibility and diagnostic performance of AccuFFRct in detecting lesion-specific ischemia in a larger cohort with FFR as the reference standard. We hypothesize that improvement in diagnostic accuracy of at least 25% for AccuFFRct as compared with CCTA. We present the article in accordance with the STARD reporting checklist (available at https://qims.amegroups.com/article/view/10.21037/qims-22-521/rc).

Methods

Study design

This is a retrospective, multi-center observational and analytical study performed at 2 sites (The Second Affiliated Hospital, Zhejiang University School of Medicine, Hangzhou, China; Zhejiang Hospital, Hangzhou, China). Adult patients who had undergone CCTA and invasive FFR measurement within 2 months were eligible for inclusion of this study. AccuFFRct analyses were performed after the enrollment and blinded to previous indexed FFR. The study was conducted in accordance with the Declaration of Helsinki (as revised in 2013). The study was approved by the Ethics Committees of The Second Affiliated Hospital, Zhejiang University School of Medicine and Zhejiang Hospital. Due to the retrospective nature of this analysis, the requirement for written informed consent was waived.

Study population

Between January 2016 and September 2017, 191 consecutive

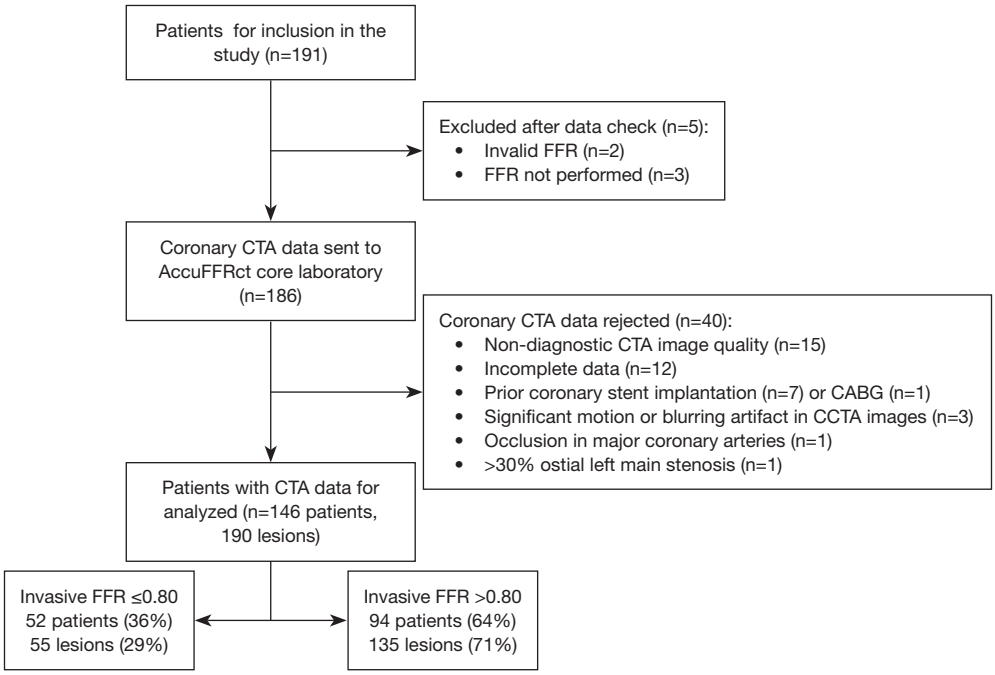

Figure 1 Flow chart of the study. CTA, computed tomography angiography; CCTA, coronary computed tomography angiography; CABG, coronary artery bypass graft; FFR, fractional flow reserve.

patients with suspected or known CAD who underwent CCTA and FFR in 60 days were included in the study. Angiographic exclusion criteria were: (I) occlusion in major coronary arteries; (II) prior stenting or coronary artery bypass grafting of the interrogated vessels; (III) significant motion or blurring artifact in CCTA images; (IV) >30% ostial left main stenosis; (V) incomplete data; (VI) non-diagnostic image quality. Thus, the final study population comprised 146 patients with 190 coronary lesions (*Figure 1*).

CCTA acquisition and analysis

Coronary angiography was performed with dual-source 128-slice CT scanners (Somatom Definition FLASH, Siemens, Forchheim, Germany). Patient with a heart rate >70 bpm received 20 mg of oral metoprolol before imaging. Sublingual sprayed nitroglycerin (0.1 mg per dose) was administered prior to scanning. During acquisition, a 60–70 mL bolus of iodinated contrast was injected at a rate of 4.0- to 4.5-mL/s, followed by a saline chaser. CCTA images were recorded with tube voltage of 120 kV, tube current of 400 mAs. The ascending aorta, coronary arteries and left ventricle should be included during CCTA acquisition. CCTA images were reconstructed with a slice thickness of 0.75 mm and an increment of 0.5 mm, using a medium/ soft kernel of B26. Two experienced radiologists blinded to ICA/FFR and AccuFFRct results visually estimated the diameter stenosis (DS%) of all coronary arteries from CCTA independently, then they would discuss and reach a consensus if there were differences. The diagnostic performance of CCTA stenosis ≥50% for detecting lesion-specific ischemia was conducted to compare with FFR with a cut-off value of 0.8. After CT examination, Angiograms were transferred to the central AccuFFRct core laboratory (ArteryFlow Technology Co., Ltd., Hangzhou, China), which were then selected for AccuFFRct computation and further analysis.

ICA and FFR measurement

Invasive coronary angiography and FFR measurement were performed by standard catheterization following societal guidelines (18,19). At least two projections were obtained per vessel distribution, with angles of projection optimized based on cardiac position. The pressure sensor was advanced past the most distal stenosis and FFR was recorded under the hyperemic condition and the location of FFR measurement was also documented. Hyperemia was attained by administering intravenous adenosine 140 μg/kg/min and FFR was automatically calculated as

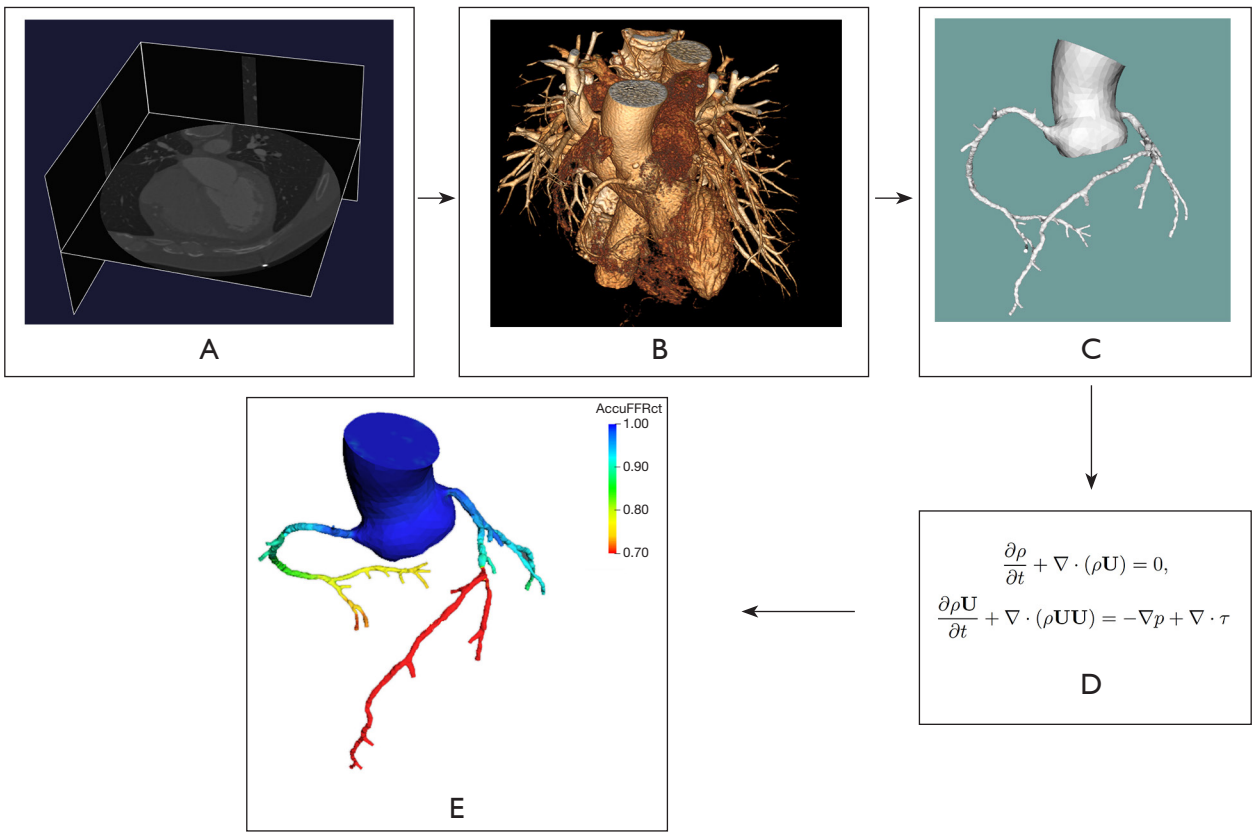

Figure 2 Workflow of AccuFFRct calculation. (A) CCTA images; (B) reconstructed 3D anatomic model; (C) segmented 3D coronary artery model; (D) CFD simulation for coronary flow and pressure distribution based on Navier-Stokes equations; (E) AccuFFRct colored distribution on the coronary artery tree. CCTA, coronary computed tomography angiography; 3D, three-dimensional; CFD, computational fluid dynamics.

the ratio of mean coronary blood pressure distal to the stenosis and mean aortic pressure at the time of the induced hyperemia. A threshold value of FFR ≤0.8 was considered hemodynamically significant and causal of ischemia.

AccuFFRct computation

The AccuFFRct was performed in a blinded fashion using a workstation-based software by core laboratory professionals (20). The workflow of the study is demonstrated in *Figure 2*.

The 3D patient-specific anatomic model including the coronary artery tree, the aorta and the heart was semi-automatically reconstructed from CCTA data. During the model reconstruction, coronary artery segmentation was performed using a convolutional neural network (CNN) based algorithm, aorta images were segmented with a U-Net based model, a Mask R-CNN segmentation method was used to extract the left ventricle. Then the final anatomic model was reconstructed based on optimized vessel borders.

The 3D segmented geometric model was first pre-processed before meshing. A volume mesh model was then generated for the computation AccuFFRct using CFD simulation with the finite volume method. For boundary conditions, the total coronary flow was calculated by the mass of the left ventricle myocardium, which could be easily obtained from CCTA-extracted myocardial volume. The relationships of mean blood flow rate and aortic pressure between the baseline value at rest condition and hyperemic value were established and used to estimate hyperemia. As for the outlets, blood flow distribution was determined by Murry's law. The arterial wall was assumed to be rigid with no-slip boundary conditions. Blood was modelled as an incompressible viscous Newtonian fluid (density ρ=1,056 kg/m^3, viscosity μ=0.0035 Pa·s) in the CFD simulation.

By solving the Navier-Stokes equations with a self-

Table 1 Patient baseline characteristics

Parameter	Number of patients [146]
Age (years)	66 [58–74]
Male sex	62 [91]
Weight (kg)	65±12
Height (cm)	164±7
Body mass index (kg/m^2)	24±3
Cardiovascular risk factors	
Systolic blood pressure (mmHg)	134±20
Diastolic blood pressure (mmHg)	76±12
Angina pectoris	21 [31]
Diabetes	19 [28]
Hypertension	60 [88]
Hyperlipidemia	12 [17]
CCTA	
CCTA stenosis ≥50% (patient)	86 [126]
AccuFFRct ≤0.80 (patient)	38 [56]
Agatston score*	
0–399	71 [71]
400–799	17 [17]
>799	12 [12]
Vessel location	
LAD	74 [108]
LCX	6 [9]
RCA	18 [26]
OM	1 [1]
Diag	1 [2]
Invasive coronary angiography	
FFR ≤0.8	36 [52]

Data are presented as median [interquartile range], mean ± standard deviation, or % [No.]. *, Agatston calcium score was only obtained in 100 patients. CCTA, coronary computed tomography angiography; LAD, left anterior descending artery; LCX, left circumflex artery; RCA, right coronary artery; OM, obtuse marginal branch; Diag, diagonal branch; FFR, fractional flow reserve.

developed specific CFD solver on a standard desktop workstation, numerical results of the flow field and pressure field of coronary arteries can be acquired and visualized on the 3D anatomic model. The AccuFFRct values were computed as the pressure ratio of the distal pressure located at the measuring point of FFR to the aortic pressure. AccuFFRct values were taken at the same position with corresponding FFR measurements for further comparison.

Statistical analysis

To detect a relative improvement in diagnostic accuracy of at least 25% for AccuFFRct as compared to CCTA, 150 vessels provided 90% power with a significance level of 0.05. All statistical analyses were performed using dedicated software (MedCalc, MedCalc Software, Mariakerke, Belgium). Continuous variables were presented as mean ± standard deviation (SD) if normally distributed, and categorical variables were presented as median [interquartile range (IQR)] or percentages. Pearson statistics and Bland-Altman plot were used to analyze the degree of correlation and agreement between AccuFFRct and invasive FFR. To assess the diagnostic performance of AccuFFRct, the diagnostic accuracy, sensitivity, specificity, positive predictive value (PPV), and negative predictive value (NPV) with their corresponding 95% confidence intervals (CIs) were calculated. The optimal threshold of AccuFFRct to determine myocardial ischemia was calculated using the Youden index. The area under the curve (AUC) was determined using the receiver operator characteristic curve analysis with 95% CI on both a per-patient and a per vessel basis. The intraobserver and interobserver variabilities in AccuFFRct analysis were performed on a randomly selected 40 cases. For the per-patient analyses, a patient was considered positive if the FFR value of any investigated vessel was ≤0.80. Statistical significance was defined as a two-sided P value of <0.05.

Results

Patient and clinical characteristics

A total of 190 vessels in 146 patients [62% men; median age: 66 (IQR, 58 to 74) years] were analyzed with AccuFFRct and compared with invasive FFR as a standard reference. The mean body mass index was 24±3 kg/m^2. The average Agatston score within the cohort of study subjects was 256.78±374.41. Out of the 190 coronary stenoses, 115 were in the left anterior descending (LAD) coronary artery, 10 of which were in the diagonal (D) branch, 21 were in the left circumflex (LCX) coronary artery, 2 were in the posterior descending (PD) and 38 lesions were in the right coronary

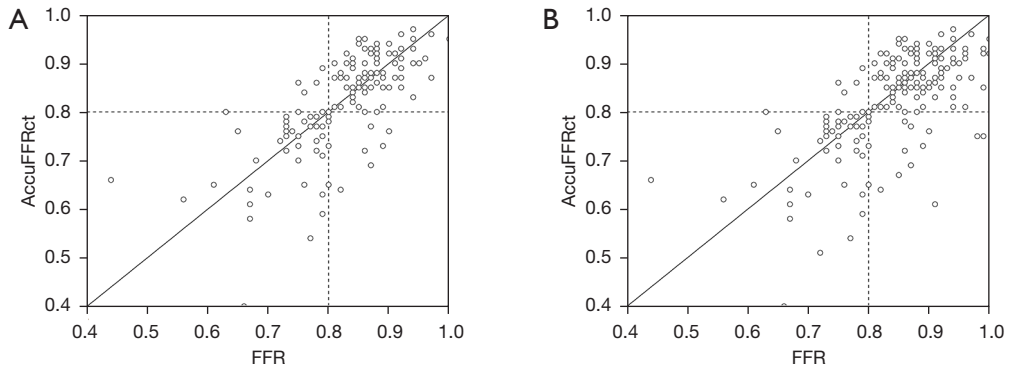

Figure 3 Correlation between FFR and AccuFFRct. Good correlations were observed on per-patient (A) (r=0.709, P<0.0001) and per-vessel (B) (r=0.655, P<0.0001) basis. FFR, fractional flow reserve.

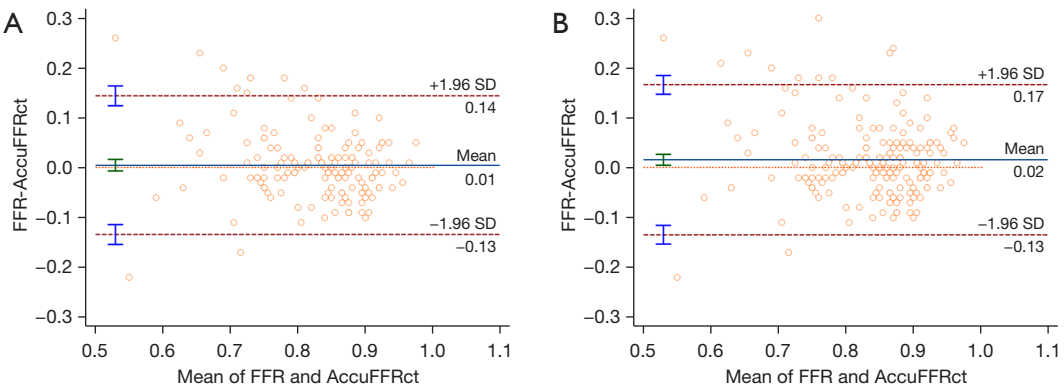

Figure 4 Agreement between FFR and AccuFFRct. Bland-Altman plot on per-patient (A) and per-vessel (B) basis showed good agreement. FFR, fractional flow reserve; SD, standard deviation.

artery (RCA). Overall, 55 stenoses (29%) were identified as hemodynamically significant based on FFR values, and the average invasive FFR was 0.84±0.09. Mean time interval between FFR and AccuFFRct was 42 (IQR, 33 to 49) months and no adverse reactions had occurred. Baseline characteristics of the study population are presented in *Table 1*.

Correlation and agreement between FFR and AccuFFRct

The optimal cut-off value for AccuFFRct was 0.80 based on the Youden's Index. The mean computed AccuFFRct was 0.82±0.10 on a per-patient basis and 0.83±0.09 on a per-vessel basis, while the mean FFR was 0.83±0.08 and 0.84±0.09, respectively. Pearson's correlation coefficient (r=0.709, P<0.001; r=0.655, P<0.001) showed that AccuFFRct correlated well with invasive FFR, and good agreement between AccuFFRct and invasive FFR was also found on both a per-patient basis (mean difference: 0.005±0.071) and a per vessel basis (mean difference: 0.016±0.077) (*Figures 3*,*4*). Representative patient case examples without and with diagnostic functional significant stenoses were shown in *Figure 5*.

Diagnostic performance of AccuFFRct

Using the threshold of FFR ≤0.80 for diagnosis of lesion-specific ischemia, AccuFFRct of 190 vessels resulted in 51 true positives, 122 true negatives, 13 false positives, and 4 false negatives. The diagnostic performance characteristics were summarized in *Table 2*. The diagnostic accuracy, sensitivity, specificity, PPV, and NPV of AccuFFRct for detecting hemodynamically significant stenoses were 91.78% (95% CI: 86.08% to 95.68%), 92.31% (95% CI: 81.46% to 97.86%), 91.49% (95% CI: 83.91% to 96.25%), 85.71% (95% CI: 75.48% to 92.12%), and 95.56% (95% CI: 89.33% to 98.22%), respectively, on the per-patient

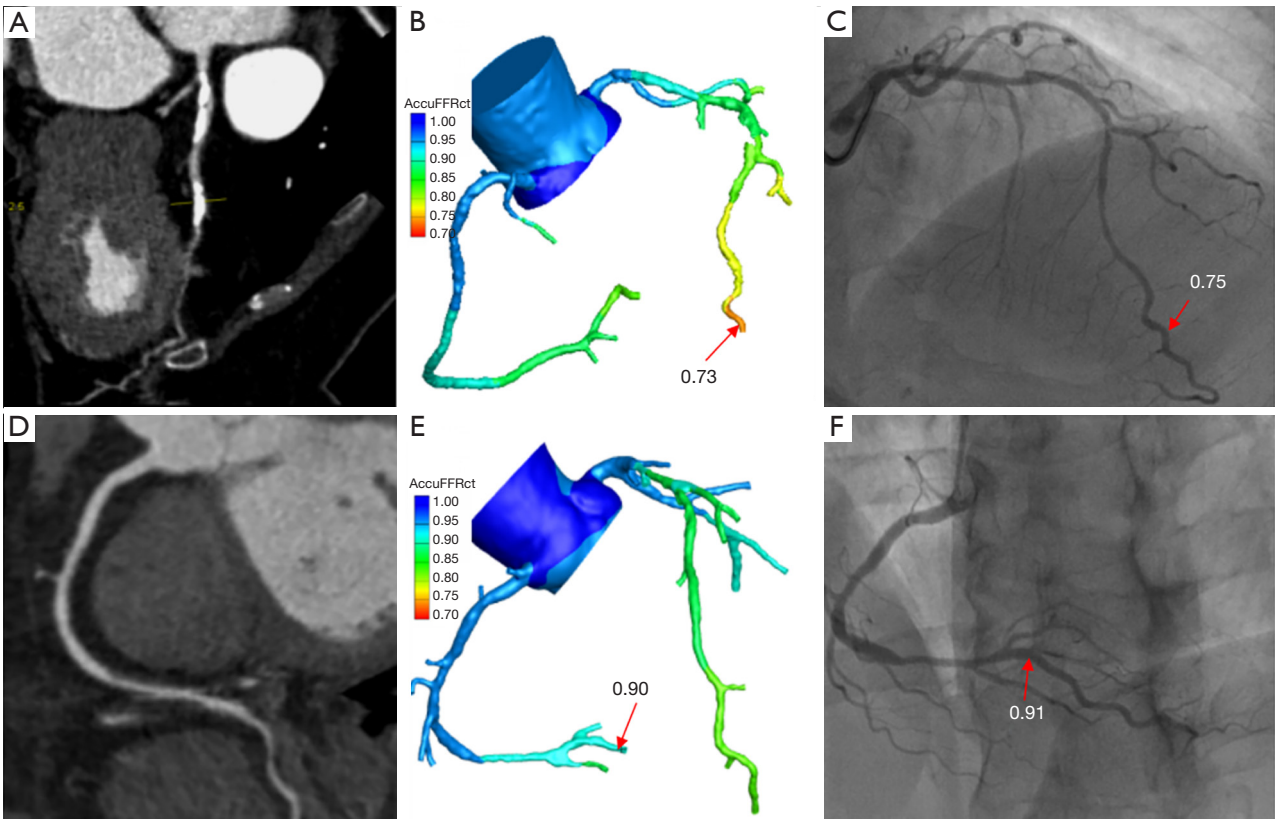

Figure 5 AccuFFRct results with invasive FFR measurement. (A) CCTA demonstrating 70% stenosis at the middle portion of LAD; (B) a computed AccuFFRct value of 0.73; (C) the corresponding measured FFR value of 0.75, demonstrating stenosis ischemia; (D) CCTA demonstrating 40% stenosis at the proximal-middle portion of RCA; (E) a computed AccuFFRct value of 0.90; (F) the corresponding measured FFR value of 0.91, indicating no stenosis ischemia. Red arrows indicate the position where FFR/AccuFFRct was measured. FFR, fractional flow reserve; CCTA, coronary computed tomography angiography; LAD, left anterior descending artery; RCA, right corona artery.

basis; on a per-vessel basis, the values were 91.05% (95% CI: 86.06% to 94.70%), 92.73% (95% CI: 82.41% to 97.98%), 90.37% (95% CI: 84.10% to 94.77%), 79.69% (95% CI: 69.95% to 86.86%) and 96.83% (95% CI: 92.22% to 98.74%), respectively. No big difference in diagnostic performance of AccuFFRct was found for all lesions and intermediate lesions.

As shown in *Figure 6*, AccuFFRct improved diagnostic performance in determining ischemia-causing lesions with an AUC of 0.935 *vs.* 0.761 (P<0.001) for patient-based assessment and 0.927 *vs.* 0.764 (P<0.001) for the vessel-based evaluation in comparison with the CCTA stenosis.

Diagnostic performance of AccuFFRct in the "gray zone"

AccuFFRct demonstrated 28 true predictions and 1 false prediction in FFR ≤0.75 "zone", 23 true and 3 false predictions in the "gray zone" (0.75< FFR ≤0.8), and 122 true predictions and 13 false predictions in FFR >0.8 "zone" on a per-vessel basis. It can be noted that the diagnostic performance of AccuFFRct for "gray zone" lesions was close to the other groups, no significant difference of discriminatory ability for functional significance was found between these 3 "zones". The diagnostic performance of AccuFFRct for different FFR "zones" is presented in *Figure* 7.

The influence of calcification

The Agatston calcium score was obtained in 100 patients, in which 71% of patients had calcium score <400, 17% had calcium score between 400 and 799, 12% had calcium score >799; and in all these patients, 37 patients (37%)

Table 2 Diagnostic performance of CCTA and AccuFFRct for the prediction of ischemia

Variables	Methods	Sensitivity (%)	Specificity (%)	PPV (%)	NPV (%)	Accuracy (%)
All lesions						
Per-patient	AccuFFRct	92.31 (81.46 to 97.86)	91.49 (83.92 to 96.25)	85.71 (75.48 to 92.12)	95.56 (89.33 to 98.22)	91.78 (86.08 to 95.68)
	CCTA	94.23 (84.05 to 98.79)	18.09 (10.90 to 27.37)	38.89 (36.16 to 41.69)	85.00 (63.53 to 94.86)	45.21 (36.96 to 53.65)
Per-vessel	AccuFFRct	92.73 (82.41 to 97.98)	90.37 (84.10 to 94.77)	79.69 (69.95 to 86.86)	96.83 (92.22 to 98.74)	91.05 (86.06 to 94.70)
	CCTA	96.36 (87.47 to 99.56)	17.04 (11.12 to 24.46)	32.12 (30.15 to 34.16)	92.00 (73.73 to 97.92)	40.00 (32.98 to 47.34)
Intermediate stenosis						
Per-patient	AccuFFRct	96.55 (82.24 to 99.91)	91.76 (83.77 to 96.62)	80.00 (66.22 to 89.08)	98.73 (91.91 to 99.81)	92.98 (86.64 to 96.92)
	CCTA	93.10 (77.23 to 99.15)	15.29 (8.40 to 24.73)	27.27 (24.70 to 30.01)	86.67 (60.92 to 96.44)	35.09 (26.38 to 44.59)
Per-vessel	AccuFFRct	96.97 (82.24 to 99.92)	90.32 (83.71 to 94.90)	72.73 (60.82 to 82.08)	99.12 (94.20 to 99.87)	91.72 (86.26 to 95.52)
	CCTA	93.94 (79.77 to 99.26)	15.32 (9.48 to 22.89)	22.79 (20.84 to 24.87)	90.48 (69.97 to 97.48)	31.85 (24.65 to 39.75)
Agatston calcium score						
Per-patient						
0–399	AccuFFRct	95.00 (75.13 to 99.87)	90.20 (78.59 to 96.74)	79.17 (62.16 to 89.78)	97.87 (87.17 to 99.68)	91.55 (82.51 to 96.84)
400–799	AccuFFRct	100.00 (63.06 to 100.00)	88.89 (51.75 to 99.72)	88.89 (55.76 to 98.07)	100.00	94.12 (71.31 to 99.85)
>799	AccuFFRct	88.89 (51.75 to 99.72)	100.00 (29.24 to 100.0)	100.00	75.00 (32.10 to 95.01)	91.67 (61.52 to 99.79)

Data are shown in percentage with 95% confidence interval in parentheses. CCTA, coronary computed tomography angiography; NPV, negative predictive value; PPV, positive predictive value.

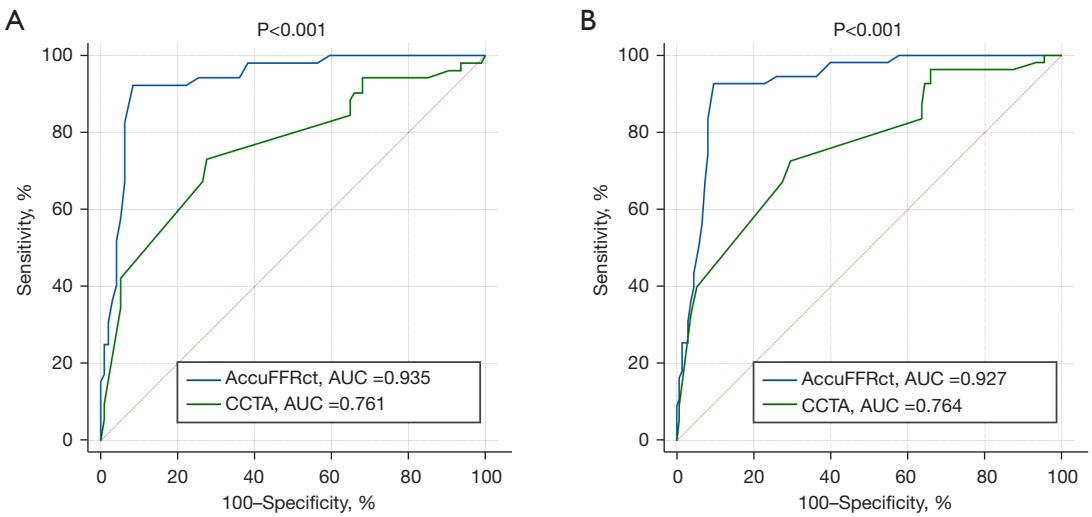

Figure 6 ROC Curves for the discrimination of functionally significant stenoses. AUC of AccuFFRct and CCTA on per-patient (A) and per-vessel (B) basis. AUC, area under the curve; CCTA, coronary computed tomography angiography; ROC, receiver operating characteristic.

were detected as functional ischemia with FFR ≤0.8. The diagnostic performance of AccuFFRct in patients with Agatston calcium scores between 0–399, 400–799, and >799 is presented in *Table 2*. One can see that there are no significant differences in diagnostic performance of AccuFFRct among these 3 groups [91.55% (95% CI: 82.51% to 96.84%) *vs.* 94.12% (95% CI: 71.31% to 99.85%) *vs.* 91.67% (95% CI: 61.52% to 99.79%)]. However, the sensitivity of calcium scores >799 group is slightly lower than the other groups, and this is

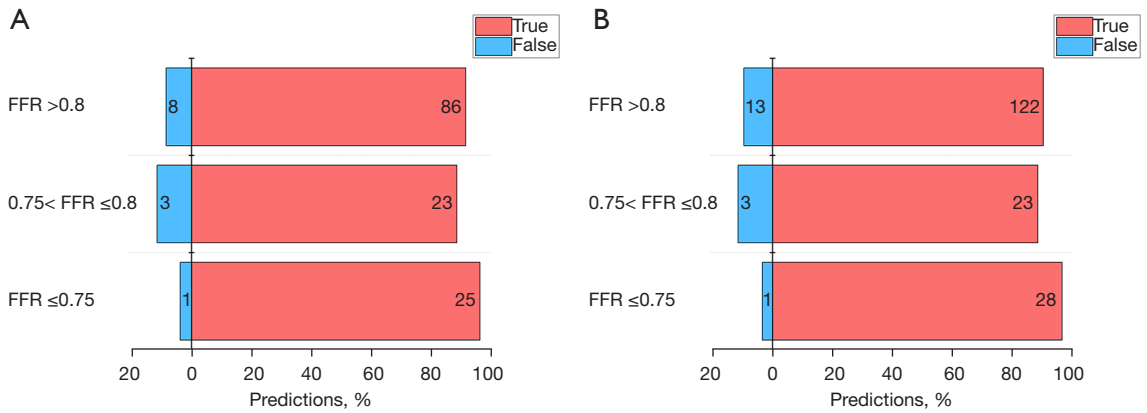

Figure 7 Diagnostic performance of AccuFFRct among different FFR zones. No significant difference between the diagnostic performance for "gray zone" lesions (0.75< FFR ≤0.8) versus the other two subgroups (FFR ≤0.75 and FFR >0.8) on per-patient (A) and per-vessel (B) basis. Number of cases were noted on bars. FFR, fractional flow reserve.

because severe calcification could affect the accuracy of reconstruction of the coronary artery model. In addition, patients with higher calcium score (>399) showed lower FFR values than the 0–399 group (0.79±0.10 *vs.* 0.84±0.07).

Computational performance of AccuFFRct

The mean operating time to compute AccuFFRct value was 30±10 min, including 3D reconstruction, meshing scheme, and the core CFD simulation on a standard desktop workstation with 4.2 GHz Intel i7 8-core processor. Intraobserver and interobserver variability in AccuFFRct analysis were 0.0±0.02 and 0.01±0.03, respectively.

Discussion

The present study demonstrates the feasibility and great diagnostic performance of a novel CT-FFR technique based on CFD analysis to allow rapid computation of FFR for evaluating the hemodynamic significance of coronary stenosis from angiographic images alone. Anatomical coronary information of a patient with suspected CAD was derived from CCTA data and then the pressure distribution affected by stenoses was obtained through CFD simulation. In our cohort of 146 patients with 190 lesions, AccuFFRct correlated well to the reference standard of invasive FFR (Pearson's correlation coefficient r=0.709, P<0.001), good agreement between AccuFFRct and the FFR measurements was also observed (mean difference: 0.005±0.071, 0.016±0.077), on both per-patient and per-vessel basis. AccuFFRct demonstrated promising potential in detecting ischemia in all lesions, including intermediate lesions, "gray zone" lesions and lesions with severe calcification.

Comparison to CCTA

When compared with CCTA alone, using DS% ≥50% as the cutoff value for CCTA-based quantitative analysis, our results showed that AccuFFRct provided superior diagnostic accuracy, 91.78% (95% CI: 86.08% to 95.68%) *vs.* 45.21% (95% CI: 36.96% to 53.65%) and 91.05% (95% CI: 86.06% to 94.70%) *vs.* 40.00% (95% CI: 32.98% to 47.34%) for per-patient and for per-vessel level, respectively. Particularly noteworthy was the marked reduction in false-positive cases when comparing AccuFFRct and CCTA diagnostic results, reduced from 112 false positives (CCTA) to 13 (AccuFFRct) on the per-vessel basis. This is in line with previous studies, which reported that overestimating stenosis severity was observed in CCTA analysis. Only a minority of CCTA-considered high-risk lesions led to ischemia (4,21). Moreover, several CCTA studies reported that the capacity of CCTA analysis for detecting hemodynamically significant coronary stenoses was very limited (12-14). These findings had provoked that anatomic analysis based only on CT angiograms may result in unnecessary ICA and PCI, which will increase patients' financial burden; functional assessment of blood flow in coronary arteries is essential for accurate evaluation of ischemia-causing lesions.

Comparison to CT-FFR

CT-derived FFR technology that allows noninvasive

assessment of FFR from standard acquired CCTA data by combining the CFD model is more cost-saving than ICA and may improve the quality of life for people with suspected CAD (22). In recent years, several CT-FFR technologies have been developed. Kim and Taylor (11,23,24) first reported a novel approach for the computation of FFR_{CT} from CCTA images. The 3D anatomic model was reconstructed from CCTA and lumped models were used for boundary conditions. In 3 clinical trials (DISCOVER-FLOW, DeFACTO and NXT), FFR_{CT} showed good diagnostic performance in identifying lesion-specific ischemia as revealed by invasive FFR, with the accuracy ranges from 73% to 86% and AUCs ranging between 0.81 and 0.90 (12-14). Furthermore, an advanced study of 5,083 patients with known or suspected CAD represented the excellent performance of FFR_{CT} for guiding clinical strategies compared to CCTA, which improved 1-year event-free survival and reduced unnecessary revascularization (25,26).

Siemens Healthcare developed a one-dimensional computational analysis technique (cFFR) using a reduced-order CFD model (27). The diagnostic accuracy for assessing ischemia of cFFR ranges from 70% to 75%, with AUCs varies from 0.83 to 0.92 (27-31). The machine learning (ML)-based cFFR is the latest version of CT derived FFR approach developed by Siemens Healthcare (32). This algorithm extracted features from CCTA images and the CFD model and was trained by flow field results. Validation studies of ML-based cFFR reported relatively good diagnostic performance with accuracy ranging from 78% to 85% and AUCs from 0.84 to 0.89 (32,33). As for another method, Toshiba (34) developed a one-dimensional algorithm for computing FFR from CCTA, with an accuracy of 84% and AUC of 0.88. A deep learning CT-FFR approach was reported lately, showing relatively high diagnostic accuracy (87%) with the AUC =0.93 (35).

Our study showed comparable diagnostic performance using AccuFFRct to categorize the physiological significance of CAD. The per-vessel diagnostic accuracy of AccuFFRct is 91.1%, which is higher than the abovementioned CT-FFR approaches. The AUC of this novel method in ischemia identification is 0.927 (P<0.001) on a per-vessel basis, the documented best AUC for FFRCT, cFFR, Toshiba CT-FFR and DEEPVESSEL-FFR is 0.93, with no significant difference.

"Gray zone" and calcification

The concept of "gray zone" indicates lesions with FFR values between 0.75 and 0.8. These lesions are generally tricky and challenging for CT-FFR to identify true positive cases. In our study, though the relatively lower diagnostic accuracy of AccuFFRct for "gray zone" lesions was also observed, its diagnostic performance was still comparable and way much better than CCTA. Additionally, one can see that only 26 out of 190 lesions were in the "gray zone", the "gray zone" diagnostic performance could be better investigated in a future study with more study population.

As for calcification in CT-FFR, AccuFFRct showed very good diagnostic performance in identifying hemodynamic significance among all lesions with different calcium scores ranging from 0 to 1,700, only a slight decrease in diagnostic accuracy was observed for lesions with calcium score >799. This is mainly due to the deep learning-based segmentation algorithm, it was trained using a database containing more than 1,000 patients' CCTA data, and it was specially optimized for segmenting calcified lesions.

These results showed great promise of AccuFFRct in being able to predict functional significant CAD in a wide range of clinical applications for different kinds of lesions.

Capability

With modified algorithms and simplified processes, the advantages of AccuFFRct are time-efficiency and cost-saving. One of the main restrictions of FFRCT is the necessity of using off-site supercomputers, which resulted in 1 to 4 hours of computing time (14). The one-dimensional CFD-based cFFR and ML-based cFFR assessment took about 20 to 50 min to obtain the FFR value (28,29,31,32,36). It should be noted that the reduced-order method can reduce the computing cost of time. At the same time, it may also reduce the flow field information and lead to reduce diagnostic performance compared to the 3D model. The novel AccuFFRct method takes 30 min for pre-processing and 5 min for 3D CFD simulation. One can see that most of the time was used for 3D reconstruction. We are developing a new deep learning algorithm that may reduce the duration of reconstruction to 5 min. Our study demonstrated a novel approach with a good balance of diagnostic accuracy and the computation time involving a 3D model, which could be computed at point-of-care.

Study limitations

The study has several inherent limitations. Study inclusion/exclusion was based on pre-specified selection criteria,

thus the results of this study cannot be generalized to all patients with suspected or known CAD. Secondly, the study population was small compared to big trials. Larger multicenter and prospective studies are required to establish the diagnostic performance of AccuFFRct further and to assess to what extent obtaining AcuFFRct measures actually improves clinical outcomes.

Conclusions

AccuFFRct measured from the CCTA provides accurate detection of the functional significance of coronary stenosis and performs well in "gray zone" lesions and in lesions with severe calcification. The diagnostic specificity of AccuFFRct is significantly improved compared with the anatomical interpretation of coronary CTA, which will contribute to the comprehensive anatomical and functional evaluation of CAD and to promote clinical outcomes in a beneficial way.

Clinical perspectives

Clinical competencies

AccuFFRct can quickly and accurately calculate non-invasive FFR values based on CCTA images only, which can be a safe, efficient, and credible tool for evaluation of coronary stenosis severity and avoid unnecessary ICA and PCI treatment. This could be very useful for medical staff in the Patient Care and Procedural Skills competency domain.

Translational outlook

AccuFFRct can be applied on-site or off-site as software or a workstation, this can accelerate the delivery of specific and the most suitable therapies to patients. The diagnostic value of this approach among a universal application should be further investigated.

Acknowledgments

Funding: This work was supported by National Natural Science Foundation of China (No. 82170332), Major Medical and Health Science and Technology Plan of Zhejiang Province (No. WKJ-ZJ-1913), Zhejiang Provincial Key Research and Development Plan (No. 2020C03016), National Natural Science Foundation of China (No. 82170329), Zhejiang Provincial Public Welfare Technology Research Project (Nos. LGF20H020012 and LGF21H020003), Major Project of Social Development of Jinhua Science and Technology Project (No. 2020-3-027), and Key Project of Social Development of Jinhua Science and Technology Project (No. 2020-3-047).

Footnote

Reporting Checklist: The authors have completed the STARD reporting checklist. Available at https://qims.amegroups.com/article/view/10.21037/qims-22-521/rc

Conflicts of Interest: All authors have completed the ICMJE uniform disclosure form (available at https://qims.amegroups.com/article/view/10.21037/qims-22-521/coif). J Jiang received grants form National Natural Science Foundation of China (Nos. 81100141, 81570322, 82170332) and Zhejiang Provincial Key Research and Development Plan (No. 2020C03016); CD received grant from Major Medical and Health Science and Technology Plan of Zhejiang Province (No. WKJ-ZJ-1913); YH is an employee of ArteryFlow; YP received grants from Zhejiang Provincial Public Welfare Technology Research Project (No. LGF21H020003) and Major Project of Social Development of Jinhua Science and Technology Project (No. 2020-3-027); LB received grant from Key Project of Social Development of Jinhua Science and Technology Project (No. 2020-3-047); LD received grant from National Natural Science Foundation of China (No. 82170329); CL received grant from Zhejiang Provincial Public Welfare Technology Research Project (No. LGF20H020012); XL is a co-founder of ArteryFlow; JX is the CEO of ArteryFlow; JAW received grant from National Natural Science Foundation of China (Nos. 81320108003, 31371498). The other authors have no conflicts of interest to declare.

Ethical Statement: The authors are accountable for all aspects of the work in ensuring that questions related to the accuracy or integrity of any part of the work are appropriately investigated and resolved. The study was conducted in accordance with the Declaration of Helsinki (as revised in 2013). The study was approved by the Ethics Committees of The Second Affiliated Hospital, Zhejiang University School of Medicine and Zhejiang Hospital, individual consent was waived for the retrospective nature of the study.

References

1. Global, regional, and national life expectancy, all-cause mortality, and cause-specific mortality for 249 causes of death, 1980-2015: a systematic analysis for the Global Burden of Disease Study 2015. Lancet 2016;388:1459-544.
2. Windecker S, Kolh P, Alfonso F, Collet JP, Cremer J, et al. 2014 ESC/EACTS Guidelines on myocardial revascularization: The Task Force on Myocardial Revascularization of the European Society of Cardiology (ESC) and the European Association for Cardio-Thoracic Surgery (EACTS)Developed with the special contribution of the European Association of Percutaneous Cardiovascular Interventions (EAPCI). Eur Heart J 2014;35:2541-619.
3. Montalescot G, Sechtem U, Achenbach S, Andreotti F, Arden C, et al. 2013 ESC guidelines on the management of stable coronary artery disease: the Task Force on the management of stable coronary artery disease of the European Society of Cardiology. Eur Heart J 2013;34:2949-3003.
4. Meijboom WB, Van Mieghem CA, van Pelt N, Weustink A, Pugliese F, Mollet NR, Boersma E, Regar E, van Geuns RJ, de Jaegere PJ, Serruys PW, Krestin GP, de Feyter PJ. Comprehensive assessment of coronary artery stenoses: computed tomography coronary angiography versus conventional coronary angiography and correlation with fractional flow reserve in patients with stable angina. J Am Coll Cardiol 2008;52:636-43.
5. Tonino PA, De Bruyne B, Pijls NH, Siebert U, Ikeno F, van' t Veer M, Klauss V, Manoharan G, Engstrøm T, Oldroyd KG, Ver Lee PN, MacCarthy PA, Fearon WF; . Fractional flow reserve versus angiography for guiding percutaneous coronary intervention. N Engl J Med 2009;360:213-24.
6. De Bruyne B, Pijls NH, Kalesan B, Barbato E, Tonino PA, Piroth Z, et al. Fractional flow reserve-guided PCI versus medical therapy in stable coronary disease. N Engl J Med 2012;367:991-1001.
7. Berry C, Corcoran D, Hennigan B, Watkins S, Layland J, Oldroyd KG. Fractional flow reserve-guided management in stable coronary disease and acute myocardial infarction: recent developments. Eur Heart J 2015;36:3155-64.
8. Fearon WF. Percutaneous coronary intervention should be guided by fractional flow reserve measurement. Circulation 2014;129:1860-70.
9. Johnson NP, Tóth GG, Lai D, Zhu H, Açar G, Agostoni P, et al. Prognostic value of fractional flow reserve: linking physiologic severity to clinical outcomes. J Am Coll Cardiol 2014;64:1641-54.
10. Ties D, van Dijk R, Pundziute G, Lipsic E, Vonck TE, van den Heuvel AFM, Vliegenthart R, Oudkerk M, van der Harst P. Computational quantitative flow ratio to assess functional severity of coronary artery stenosis. Int J Cardiol 2018;271:36-41.
11. Kim HJ, Vignon-Clementel IE, Coogan JS, Figueroa CA, Jansen KE, Taylor CA. Patient-specific modeling of blood flow and pressure in human coronary arteries. Ann Biomed Eng 2010;38:3195-209.
12. Koo BK, Erglis A, Doh JH, Daniels DV, Jegere S, Kim HS, Dunning A, DeFrance T, Lansky A, Leipsic J, Min JK. Diagnosis of ischemia-causing coronary stenoses by noninvasive fractional flow reserve computed from coronary computed tomographic angiograms. Results from the prospective multicenter DISCOVER-FLOW (Diagnosis of Ischemia-Causing Stenoses Obtained Via Noninvasive Fractional Flow Reserve) study. J Am Coll Cardiol 2011;58:1989-97.
13. Min JK, Leipsic J, Pencina MJ, Berman DS, Koo BK, van Mieghem C, Erglis A, Lin FY, Dunning AM, Apruzzese P, Budoff MJ, Cole JH, Jaffer FA, Leon MB, Malpeso J, Mancini GB, Park SJ, Schwartz RS, Shaw LJ, Mauri L. Diagnostic accuracy of fractional flow reserve from anatomic CT angiography. JAMA 2012;308:1237-45.
14. Nørgaard BL, Leipsic J, Gaur S, Seneviratne S, Ko BS, Ito H, et al. Diagnostic performance of noninvasive fractional flow reserve derived from coronary computed tomography angiography in suspected coronary artery disease: the NXT trial (Analysis of Coronary Blood Flow Using CT Angiography: Next Steps). J Am Coll Cardiol 2014;63:1145-55.
15. Nørgaard BL, Hjort J, Gaur S, Hansson N, Bøtker HE, Leipsic J, Mathiassen ON, Grove EL, Pedersen K, Christiansen EH, Kaltoft A, Gormsen LC, Mæng M, Terkelsen CJ, Kristensen SD, Krusell LR, Jensen JM. Clinical Use of Coronary CTA-Derived FFR for Decision-Making in Stable CAD. JACC Cardiovasc Imaging 2017;10:541-50.
16. Douglas PS, De Bruyne B, Pontone G, Patel MR, Norgaard BL, Byrne RA, et al. 1-Year Outcomes of

FFRCT-Guided Care in Patients With Suspected Coronary Disease: The PLATFORM Study. J Am Coll Cardiol 2016;68:435-45.
17. Tesche C, De Cecco CN, Albrecht MH, Duguay TM, Bayer RR 2nd, Litwin SE, Steinberg DH, Schoepf UJ. Coronary CT Angiography-derived Fractional Flow Reserve. Radiology 2017;285:17-33.
18. Neumann FJ, Sousa-Uva M, Ahlsson A, Alfonso F, Banning AP, Benedetto U, et al. 2018 ESC/EACTS Guidelines on myocardial revascularization. Eur Heart J 2019;40:87-165.
19. Lawton JS, Tamis-Holland JE, Bangalore S, Bates ER, Beckie TM, et al. 2021 ACC/AHA/SCAI Guideline for Coronary Artery Revascularization: A Report of the American College of Cardiology/American Heart Association Joint Committee on Clinical Practice Guidelines. J Am Coll Cardiol 2022;79:e21-e129.
20. Jiang W, Pan Y, Hu Y, Leng X, Jiang J, Feng L, Xia Y, Sun Y, Wang J, Xiang J, Li C. Diagnostic accuracy of coronary computed tomography angiography-derived fractional flow reserve. Biomed Eng Online 2021;20:77.
21. Goldstein JA, Gallagher MJ, O'Neill WW, Ross MA, O'Neil BJ, Raff GL. A randomized controlled trial of multi-slice coronary computed tomography for evaluation of acute chest pain. J Am Coll Cardiol 2007;49:863-71.
22. Kishi S, Giannopoulos AA, Tang A, Kato N, Chatzizisis YS, Dennie C, Horiuchi Y, Tanabe K, Lima JAC, Rybicki FJ, Mitsouras D. Fractional Flow Reserve Estimated at Coronary CT Angiography in Intermediate Lesions: Comparison of Diagnostic Accuracy of Different Methods to Determine Coronary Flow Distribution. Radiology 2018;287:76-84.
23. Kim HJ, Vignon-Clementel IE, Figueroa CA, LaDisa JF, Jansen KE, Feinstein JA, Taylor CA. On coupling a lumped parameter heart model and a three-dimensional finite element aorta model. Ann Biomed Eng 2009;37:2153-69.
24. Taylor CA, Fonte TA, Min JK. Computational fluid dynamics applied to cardiac computed tomography for noninvasive quantification of fractional flow reserve: scientific basis. J Am Coll Cardiol 2013;61:2233-41.
25. Fairbairn TA, Nieman K, Akasaka T, Nørgaard BL, Berman DS, Raff G, et al. Real-world clinical utility and impact on clinical decision-making of coronary computed tomography angiography-derived fractional flow reserve: lessons from the ADVANCE Registry. Eur Heart J 2018;39:3701-11.
26. Patel MR, Nørgaard BL, Fairbairn TA, Nieman K, Akasaka T, Berman DS, et al. 1-Year Impact on Medical Practice and Clinical Outcomes of FFR(CT): The ADVANCE Registry. JACC Cardiovasc Imaging 2020;13:97-105.
27. Coenen A, Lubbers MM, Kurata A, Kono A, Dedic A, Chelu RG, Dijkshoorn ML, Gijsen FJ, Ouhlous M, van Geuns RJ, Nieman K. Fractional flow reserve computed from noninvasive CT angiography data: diagnostic performance of an on-site clinician-operated computational fluid dynamics algorithm. Radiology 2015;274:674-83.
28. Coenen A, Rossi A, Lubbers MM, Kurata A, Kono AK, Chelu RG, Segreto S, Dijkshoorn ML, Wragg A, van Geuns RM, Pugliese F, Nieman K. Integrating CT Myocardial Perfusion and CT-FFR in the Work-Up of Coronary Artery Disease. JACC Cardiovasc Imaging 2017;10:760-70.
29. Coenen A, Lubbers MM, Kurata A, Kono A, Dedic A, Chelu RG, Dijkshoorn ML, van Geuns RJ, Schoebinger M, Itu L, Sharma P, Nieman K. Coronary CT angiography derived fractional flow reserve: Methodology and evaluation of a point of care algorithm. J Cardiovasc Comput Tomogr 2016;10:105-13.
30. Renker M, Schoepf UJ, Wang R, Meinel FG, Rier JD, Bayer RR 2nd, Möllmann H, Hamm CW, Steinberg DH, Baumann S. Comparison of diagnostic value of a novel noninvasive coronary computed tomography angiography method versus standard coronary angiography for assessing fractional flow reserve. Am J Cardiol 2014;114:1303-8.
31. Baumann S, Wang R, Schoepf UJ, Steinberg DH, Spearman JV, Bayer RR 2nd, Hamm CW, Renker M. Coronary CT angiography-derived fractional flow reserve correlated with invasive fractional flow reserve measurements--initial experience with a novel physician-driven algorithm. Eur Radiol 2015;25:1201-7.
32. Tesche C, De Cecco CN, Baumann S, Renker M, McLaurin TW, Duguay TM, Bayer RR 2nd, Steinberg DH, Grant KL, Canstein C, Schwemmer C, Schoebinger M, Itu LM, Rapaka S, Sharma P, Schoepf UJ. Coronary CT Angiography-derived Fractional Flow Reserve: Machine Learning Algorithm versus Computational Fluid Dynamics Modeling. Radiology 2018;288:64-72.
33. Coenen A, Kim YH, Kruk M, Tesche C, De Geer J, Kurata A, Lubbers ML, Daemen J, Itu L, Rapaka S, Sharma P, Schwemmer C, Persson A, Schoepf UJ, Kepka C, Hyun Yang D, Nieman K. Diagnostic Accuracy of a Machine-Learning Approach to Coronary Computed Tomographic Angiography-Based Fractional Flow Reserve: Result From the MACHINE Consortium. Circ Cardiovasc Imaging

2018;11:e007217.
34. Ko BS, Cameron JD, Munnur RK, Wong DTL, Fujisawa Y, Sakaguchi T, Hirohata K, Hislop-Jambrich J, Fujimoto S, Takamura K, Crossett M, Leung M, Kuganesan A, Malaiapan Y, Nasis A, Troupis J, Meredith IT, Seneviratne SK. Noninvasive CT-Derived FFR Based on Structural and Fluid Analysis: A Comparison With Invasive FFR for Detection of Functionally Significant Stenosis. JACC Cardiovasc Imaging 2017;10:663-73.
35. Wang ZQ, Zhou YJ, Zhao YX, Shi DM, Liu YY, Liu W, Liu XL, Li YP. Diagnostic accuracy of a deep learning approach to calculate FFR from coronary CT angiography. J Geriatr Cardiol 2019;16:42-8.
36. Kruk M, Wardziak Ł, Demkow M, Pleban W, Pręgowski J, Dzielińska Z, Witulski M, Witkowski A, Rużyłło W, Kępka C. Workstation-Based Calculation of CTA-Based FFR for Intermediate Stenosis. JACC Cardiovasc Imaging 2016;9:690-9.

Cite this article as: Jiang J, Du C, Hu Y, Yuan H, Wang J, Pan Y, Bao L, Dong L, Li C, Sun Y, Leng X, Xiang J, Tang L, Wang J. Diagnostic performance of computational fluid dynamics (CFD)-based fractional flow reserve (FFR) derived from coronary computed tomographic angiography (CCTA) for assessing functional severity of coronary lesions. Quant Imaging Med Surg 2023;13(3):1672-1685. doi: 10.21037/qims-22-521

